

## Elastic Scattering of Partially Coherent Beams of Fast Electrons in a Perfect Crystal

N. I. BORGARDT

*Moscow Institute of Electronic Technology, 103498 Moscow, Russia*

*(Received 19 August 1995; accepted 6 June 1996)*

### Abstract

Scattering of a quasi-monochromatic electron beam emitted by an extended source by a crystal is described with the use of the mutual coherency function and formalism Bloch waves. An expression correlating the mutual intensities on the exit and entrance surfaces of the crystal under partially coherent illumination is obtained. The case of illumination by an effective incoherent source filling the condenser aperture is considered. The effect of coherence of an incident beam on the intensity distribution in electron-microscopy images has been studied. For a wedge-shaped crystal, intensity profiles of a transmitted electron beam in images obtained at different values of incident-beam divergency and defocusing of the objective lens have been calculated.

### 1. Introduction

In a theoretical description of the diffraction of electrons with an energy higher than 100 keV in a crystal, the incident-particle wave function is usually presented as a plane wave. This implies that a point source of the illumination system irradiates the specimen with a parallel monochromatic beam of non-interacting particles. Although such an approximation is an idealization of actual illumination, it is successfully used in many applications, *e.g.* for interpretation of images with a diffraction contrast.

However, the incident plane-wave approximation is insufficient for simulating high-resolution electron microscopy images. Frank (1973), Wade & Frank (1977), Fejes (1977), Hawkes (1978), Ishizuka (1980) and Humphreys & Spence (1981) have investigated the effect of finite sizes of the source and the energy spread of incident particles for such images. Charges in the microscope transfer function caused by incoherent illumination have mainly been analyzed in these investigations. For the specimen transmission function, the authors have used the approximation of a 'thin' object within the limits of which the scattering differences in plane waves falling at different angles are not taken into account. Differences within the framework of the perturbation method were taken into account by Coene, Van Dyck & Van Landaut (1986). The above approximations for the specimen transmis-

sion function are valid for crystals some tens of nanometers thick, and they cannot be used in the general case. To overcome the shortcomings of the 'thin' object approximation, Rose (1984) proposed using the mutual dynamic object spectrum to describe electron scattering. Calculations of the spectrum, however, were made only for weakly scattering specimens and for thin phase objects.

In simulations of convergent-beam electron diffraction patterns, it is generally assumed that the specimen is illuminated by an effective incoherent source filling the condenser aperture (incoherent illumination). In this case, it is believed that the plane waves falling on the crystal at different angles within the limits of the illumination cone are uncorrelated (Spence & Zuo, 1992). This approximation is also used for taking into account the divergency of an incident beam in simulating defect images, *e.g.* similar calculations were carried out by Katerbau (1981) to find the diffraction contrast of small dislocation loops, and by Bithell, Donovan & Stobbs (1989) in calculating the stacking-fault images in a weak beam. Chou, Preston & Steeds (1992) used this approximation in simulating the dislocation contrast in large-angle convergent-beam electron diffraction patterns. Although the approximation of uncorrelated plane waves is widely used, its accuracy depends upon the conditions of illumination and the formation of images and also upon the crystal defects.

When the specimen is illuminated by an extended source of electrons, the incident beam appears to be a mixed ensemble of particles. To describe these ensembles, the density matrix is used in quantum mechanics (Blum, 1981). Its evolution is determined by the Liouville equation, which is derived from the Schrödinger equation. Formalism of the density matrix in the theory of scattering of fast particles in a crystal has been used in a number of papers. Kagan & Kononetz (1970, 1973) described channeling of positively charged particles (protons) in a crystal. Rez (1978) and Dudarev & Ryazanov (1988) proposed a formulation of the dynamic theory of scattering of electrons taking into account their inelastic interaction with the crystal. Wright & Bird (1992) used the density matrix for a qualitative analysis of the correlation between the waves appearing due to thermal diffusion scattering of a fast electron in a crystal. Nevertheless, it is very difficult to determine the density matrix from the

Liouville equation in the multibeam case as it requires a solution of  $N^2$  equations, where  $N$  is the quantity of diffracted beams to be taken into consideration.

Recently, Dudarev, Peng & Whelan (1993) have obtained an integral equation for the density matrix by using Green's function for the problem of an electron scattering in the crystal. Such an approach made it possible to take into account the effect of multiple inelastic scattering by collective electronic excitation in calculating the intensity distribution in the convergent-beam electron diffraction patterns.

In the above studies, formalism of the density matrix was used to describe the interaction of an individual particle with the crystal. Its wavefunction on the entrance surface of the specimen was presented as an incident plane wave. Therefore, the results obtained cannot be used directly to analyze scattering of the electron beam emitted by an extended source.

To describe the diffraction of electrons in the crystal under partially coherent illumination, it is possible to use an approach differing from that of the solution of equations for the density matrix (Borgardt, 1993a). As a matter of fact, it should describe scattering of each electron and subsequently take into account the coherent properties of the beam of particles falling on the crystal. The advantage of such an approach follows from the fact that methods of determination of the electron wavefunction in a crystal are well developed. To characterize the electron beam, we have used the mutual coherence function and the mutual intensity function conventionally applied in electron microscopy. Similarly to the density matrix, these functions make it possible to determine the time-average intensity distribution both in an electron-microscopy image and in a diffraction pattern.

The above approach is consistently described in the present work. §2 presents a definition of mutual coherence and mutual intensity functions for the electron beam and their values on the crystal entrance surface are calculated. Propagation of mutual intensity through a perfect crystal is described in §3. §4 presents an analysis of the effect of the coherence of incident electron waves on the thickness oscillations of the transmitted-beam intensity that appear after scattering by a wedge-shaped crystal. §5 gives the conclusion.

## 2. Mutual intensity on crystal entrance surface

In transmission electron microscopes, the specimens investigated are irradiated by a quasi-monochromatic beam of fast electrons whose average energy  $E_0$  is a hundred or more keV. The differences between the energy of separate electrons and  $E_0$  determine the beam energy width, which depends upon the design of the electron gun and is within the range  $\Delta E \leq 1.5$  eV. The spread is due to the Maxwell distribution of velocities of particles emitted by the source (cathode), the Boersch

effect (Boersch, 1954) caused by interactions between the electrons of the beam and instabilities of a high accelerating voltage.

To describe the electron motion, we bring into coincidence the origin of the Cartesian system of coordinates with the point of intersection of the microscope optical axis with the entrance surface of the crystal, while axis  $z$  is directed along the normal to the surface deep into the crystal. We make the origin of coordinates in the reciprocal space coincident with one of the points of the reciprocal lattice, while axes  $k_x, k_y, k_z$  are chosen to be parallel to the corresponding axes of the real space (Fig. 1). Let us assume that the  $i$ th element of the surface of source  $\Delta\sigma_i$  at time  $t_i$  starts emitting an electron whose energy is equal to  $E_i$ . From quantum mechanics, it follows that each emitted particle appears owing to disintegration of the system comprising the source and the electron inside it. Therefore, the energy of each emitted particle is determined with an accuracy of  $\delta E$  in the vicinity of the value of  $E_i$ . The  $\delta E$  value is related to the time of emission of the electron by source  $\tau_e$  based on the relationship  $\delta E \tau_e \sim h$ , where  $h$  is Planck's constant (Landau & Lifschitz, 1977). Approximate calculations show that  $\delta E$  is small compared to the beam energy width  $\Delta E$ . The precise value of  $\delta E$  is insignificant and therefore it is not calculated.

At low current densities of the beam, the Boersch effect can be neglected and, to describe the motion of

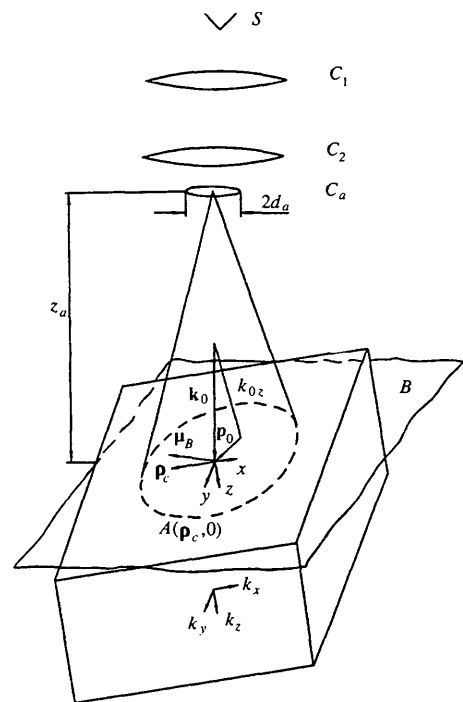


Fig. 1. Crystal specimen illuminated by a partially coherent beam of electrons.  $S$  is the electron source,  $C_1$ ,  $C_2$  are condenser lenses,  $C_a$  a condenser aperture,  $B$  the plane perpendicular to the optic axis and passing through the origin of coordinates.

each of the electrons, the single-particle wavefunction  $\Psi(\mathbf{r}, t, i) \equiv \Psi(\mathbf{r}, \Delta\sigma_i, t, t_i)$  can be used. It describes the wave package that propagates from the electron source through the specimen to the microscope screen. The square of the function modulus determines the density of the probability of a particle emitted by the source element  $\Delta\sigma_i$  at time  $t_i$  being at the point  $\mathbf{r}$  at time  $t$ .

Assuming the incident electron beam to be stationary, we introduce the function of mutual coherence, which characterizes its correlations in points  $\mathbf{r}_1$  and  $\mathbf{r}_2$  at the moment  $t + \tau$  and  $t$ , respectively:

$$\Gamma(\mathbf{r}_1, \mathbf{r}_2, \tau) = \left\langle \sum_i \sum_{i'} \Psi(\mathbf{r}_1, t + \tau, i) \Psi^*(\mathbf{r}_2, t, i') \right\rangle, \quad (1)$$

where  $\langle \rangle$  denotes the time average.

Expression (1) differs from that used to define the mutual coherence function in optics (Born & Wolf, 1968). Although the optical definition of the mutual coherence is extensively used in electron microscopy [see *e.g.* Hawkes (1978) for a review], it is not quite correct since electron waves, unlike electromagnetic waves, do not allow a determination of the function that describes a disturbance at point  $\mathbf{r}$  varying in time and appearing owing to all elements of the source. The mutual coherence function introduced by (1) makes it possible on the one hand to avoid this difficulty and on the other hand, as is seen below, it characterizes the electron beam as it does to its optical analog.

For quasi-monochromatic beams, the time lag  $\tau$  is usually much shorter than the time of the electron beam coherence  $\tau_c = h/\Delta E$ . In these cases, the expression for the mutual coherence function can be simplified and written as

$$\Gamma(\mathbf{r}_1, \mathbf{r}_2, \tau) = J(\mathbf{r}_1, \mathbf{r}_2) \exp(-2\pi i E_0 \tau / h), \quad (2)$$

where  $J(\mathbf{r}_1, \mathbf{r}_2) = \Gamma(\mathbf{r}_1, \mathbf{r}_2, 0)$  is the mutual intensity characterizing the beam spatial coherence.

Based on the mutual intensity function, the average beam intensity at point  $\mathbf{r}$  is calculated using

$$I(\mathbf{r}) = J(\mathbf{r}, \mathbf{r}), \quad (3)$$

which for the pure ensemble is equivalent to the intensity definition used in electron microscopy.

Let us calculate the mutual intensity of points  $\mathbf{r}_{c1}$  and  $\mathbf{r}_{c2}$  on the entrance surface of the crystal. Having used the wave functions of the stationary states, we obtain for  $\Psi_V(\mathbf{r}, t, i)$  in a vacuum

$$\Psi_V(\mathbf{r}, t, i) = \int \Psi_{VS}(\mathbf{r}, E, i) \exp(-2\pi i E t / h) dE, \quad (4)$$

where the function  $\Psi_{VS}(\mathbf{r}, E, i)$  is the product of the eigenfunction of the energy operator and the amplitude of the state corresponding to the energy  $E$ . It is not equal to zero if  $E$  differs from  $E_i$  by the order of  $\delta E$ . The fact that no limits are seen for the integral here and in what follows means that the range of possible values of the integration variable is unlimited.

We introduce the impulse-response function (Green's function)  $K(\mathbf{r}_c, \mathbf{r}_s, E)$  of the microscope illumination system, which is equal to the stationary-state amplitude of the electron wavefunction with energy  $E$  at point  $\mathbf{r}_c$  when its wavefunction at point  $\mathbf{r}_s$  of the source has unit amplitude. Then, using (4), we have

$$\begin{aligned} \Psi_V(\mathbf{r}_c, t, i) = & \iint_{\Delta\sigma_i} K(\mathbf{r}_c, \mathbf{r}_s, E) \Psi_{VS}(\mathbf{r}_s, E, i) \\ & \times \exp(-2\pi i E t / h) d\sigma dE, \end{aligned} \quad (5)$$

where  $d\sigma$  is the surface element.

Substituting (5) into (1) and integrating first with respect to time and then with respect to energy, we obtain for the mutual intensity on the entrance surface of the crystal

$$\begin{aligned} J_c(\mathbf{r}_{c1}, \mathbf{r}_{c2}) = & \lim_{T \rightarrow \infty} (1/T) \sum_i \sum_{i'} \int_{\Delta\sigma_i} \int_{\Delta\sigma_{i'}} h K(\mathbf{r}_{c1}, \mathbf{r}_{s1}, E) \\ & \times \Psi_{VS}(\mathbf{r}_{s1}, E, i) K^*(\mathbf{r}_{c2}, \mathbf{r}_{s2}, E) \\ & \times \Psi_{VS}^*(\mathbf{r}_{s2}, E, i') d\sigma_1 d\sigma_2 dE. \end{aligned} \quad (6)$$

Further on we assume that the source of electrons is incoherent. This assumption is valid in most cases and it implies that processes of emitting electrons are independent of one another. Therefore, in (6), only those terms for which  $i = i'$  are non-zero. Formally, this conclusion can be obtained if in calculation of (6) we take into account that functions  $\Psi_{VS}(\mathbf{r}_s, E, i)$  comprise a quickly oscillating multiplier  $\exp(2\pi i E t_i / h)$ , whose appearance is determined by the diversity in time of the emission of particles by the cathode. Owing to this multiplier, the effect of terms with  $i \neq i'$  becomes negligible after integration with respect to the energy.

For an incoherent source, the location of the  $\Delta\sigma_i$  regions on its surface is random. Hence, in (6), the phase factors of the product of the wave functions, which are not zero at  $\mathbf{r}_{s1} \neq \mathbf{r}_{s2}$ , are independent of each other for different terms. Therefore, for the particle ensemble, the contribution into the integral value is made by points  $\mathbf{r}_{s2}$  located within the coherence region in the vicinity of  $\mathbf{r}_{s1}$ . Since the region is many times smaller than the size of the incoherent source, one can approximately assume

$$\Psi_{VS}(\mathbf{r}_{s1}, E, i) \Psi_{VS}(\mathbf{r}_{s2}, E, i) \simeq \delta(\mathbf{r}_{s1} - \mathbf{r}_{s2}), \quad (7)$$

where  $\delta(\mathbf{r})$  is Dirac's delta-function.

Taking into account the above remarks, we can write (6) as

$$\begin{aligned} J_c(\mathbf{r}_{c1}, \mathbf{r}_{c2}) = & S_s \iint_{\sigma_s} K(\mathbf{r}_{c1}, \mathbf{r}_s, E) \\ & \times K^*(\mathbf{r}_{c2}, \mathbf{r}_s, E) I'_s(\mathbf{r}_s, E) d\sigma dE, \end{aligned} \quad (8)$$

where  $I'_s(\mathbf{r}_s, E)$  is the average intensity for electrons with energy  $E$ ,  $\sigma_s$  is the surface of the source and  $S_s$  is a constant having dimensions of area.

The constant  $S_s$  ensures the equality of (6) and (8) when (7) is used. It determines the intensity level and does not influence the spatial structure of  $J_c(\mathbf{r}_{c1}, \mathbf{r}_{c2})$ . Since for a quasi-monochromatic beam the dependence of the product of the response functions on the energy within the beam energy width  $E$ , as a rule, can be neglected, we obtain

$$J_c(\mathbf{r}_{c1}, \mathbf{r}_{c2}) = S_s \int_{\sigma_s} K(\mathbf{r}_{c1}, \mathbf{r}_s, E_0) K^*(\mathbf{r}_{c2}, \mathbf{r}_s, E_0) I_s(\mathbf{r}_s) d\sigma_s, \quad (9)$$

where  $I_s(\mathbf{r}_s) = \int I(\mathbf{r}_s, E) dE$ .

Expressions (8) and (9) together with (2) allow one to characterize the coherent properties of the electron beam falling on the specimen, based on Green's function of the optic system and a general idea of the source of particles. They are similar to the corresponding formulae used in optics (Born & Wolf, 1968). It also follows from the above analysis and the laws of propagation of mutual intensity in a vacuum that their passage through lenses is the same for both electromagnetic and electron waves. If (8) and (9) are normalized, the functions in the left-hand parts are equivalent to a time-averaged density matrix of an incident beam of electrons in  $x$  presentation.

When determining the mutual intensity on the entrance surface of the specimen, in many cases one can assume that the cathode intermediate image located before the condenser aperture (between lenses  $C_1$  and  $C_2$  in Fig. 1) is an effective incoherent electron source. The applicability of such an approximation can be estimated on the basis of the parameters of the optic system of the microscope. In this case, the response function  $K(\mathbf{r}_c, \mathbf{r}_s, E_0)$  is determined conventionally by describing the propagation of the electron wave from the cathode to the lens, its passage through the lens and condenser aperture, and its further propagation to the specimen. The corresponding formulae are given, for example, by Cowley (1975). Another possibility of determining  $J_c(\mathbf{r}_{c1}, \mathbf{r}_{c2})$  is a direct description of the propagation of mutual intensity from the source to the specimen. Such an approach is well known in optics (Goodman, 1985).

Calculation of mutual intensity is simplified in the case of incoherent critical illumination. We assume that the microscope illumination system with the condenser aperture at the end focuses the source image on the plane  $B$ , which is perpendicular to the optical axis and passes through the origin (Fig. 1). If the source image on plane  $B$  is a homogeneously illuminated circle with radius  $d_B$ , the coherence length in the condenser aperture plane is determined according to Spence (1988) by the formula

$$l_{sa} = \lambda_0 z_a / 2\pi d_B,$$

where  $\lambda_0 = \lambda(E_0)$  is the electron wavelength calculated with the relativistic corrections taken into account, and

$z_a$  is the distance between the condenser aperture and plane  $B$ .

In the cases when the length  $l_{sa}$  is much smaller than the aperture size, one can assume that it is an effective incoherent source of electrons, whose intensity has the form

$$I_a(\boldsymbol{\mu}_a) = I_{0a} s_a(\boldsymbol{\mu}_a), \quad (10)$$

where  $\boldsymbol{\mu}_a$  is a vector in the aperture plane,  $I_{0a}$  is constant, and  $s_a(\boldsymbol{\mu}_a)$  is the form function determined by the expression

$$s_a(\boldsymbol{\mu}_a) = \begin{cases} 1 & \text{for } \mu_a \leq d_a \\ 0 & \text{for } \mu_a > d_a, \end{cases}$$

where  $d_a$  is the radius of the aperture.

The function  $K(\mathbf{r}, \mathbf{r}_a, E_0)$  when incoherent illumination is used is determined by the formula

$$K(\mathbf{r}, \mathbf{r}_a, E_0) = \exp(2\pi i |\mathbf{r} - \mathbf{r}_a| / \lambda_0) / (i \lambda_0 |\mathbf{r} - \mathbf{r}_a|). \quad (11)$$

The mutual intensity  $J_B(\boldsymbol{\mu}_{B1}, \boldsymbol{\mu}_{B2})$  on the plane  $B$  can be presented as

$$J_B(\boldsymbol{\mu}_{B1}, \boldsymbol{\mu}_{B2}) = I_B J'(\boldsymbol{\mu}_{B1}, \boldsymbol{\mu}_{B2}) s_B(\boldsymbol{\mu}_{B1}) s_B(\boldsymbol{\mu}_{B2}), \quad (12)$$

where  $\boldsymbol{\mu}_B$  is a vector in the  $B$  plane,  $s_B(\boldsymbol{\mu}_B)$  is the form function of the illuminated region equal to unity at  $\mu_B \leq d_B$  and to zero at  $\mu_B > d_B$ , and  $I_B$  is a constant determined from the equality of the electron flow through the condenser aperture and plane  $B$ .

Function  $J'(\boldsymbol{\mu}_{B1}, \boldsymbol{\mu}_{B2})$  is determined on the basis of the van Cittert-Zernike theorem and given by the formula

$$J'(\boldsymbol{\mu}_{B1}, \boldsymbol{\mu}_{B2}) = [\exp(i\pi\phi) / \pi d_a^2] \int s_a(\boldsymbol{\mu}_a) \times \exp[-(2\pi i / \lambda_0 z_a)(\boldsymbol{\mu}_{B1} - \boldsymbol{\mu}_{B2}) \cdot \boldsymbol{\mu}_a] d\boldsymbol{\mu}_a, \quad (13)$$

where  $\phi = (\mu_{B1}^2 - \mu_{B2}^2) / \lambda_0 z_a$ .

This expression is directly obtained as a result of substituting (10) and (11) into (9), use of the approximation of the Fresnel diffraction, and introduction of the normalization factor. After integration, we get

$$J'(\boldsymbol{\mu}_{B1}, \boldsymbol{\mu}_{B2}) = [2J_1(X) / X] \exp(i\pi\phi), \quad (14)$$

where  $X = 2\pi\theta_a |\boldsymbol{\mu}_{B1} - \boldsymbol{\mu}_{B2}| / \lambda_0$ ,  $\theta_a \simeq d_a / z_a$  is a semi-angle of the incident-beam divergency and  $J_1(X)$  is the first-order Bessel function.

Function  $J'(\boldsymbol{\mu}_{B1}, \boldsymbol{\mu}_{B2})$  is equal to unity at  $\boldsymbol{\mu}_{B1} = \boldsymbol{\mu}_{B2}$  and rapidly decreases to a small value at  $|\boldsymbol{\mu}_{B1} - \boldsymbol{\mu}_{B2}| > l_s$ , where  $l_s = \lambda_0 / 2\pi\theta_a$  is a coherency length in plane  $B$ .

Expressions (12) and (14) determine the mutual intensity in the plane  $B$  when no lenses are used between the condenser aperture and the specimen. The illumination system of modern microscopes has additional lenses that make it possible to considerably decrease the size of the illuminated area. However, the size of the exit pupil of such systems is still determined

by the diameter of the condenser aperture as before. Then the mutual intensity function of the spot focused on the specimen differs from the mutual intensity in an intermediate image of the source placed behind the aperture only in that its arguments have a scale factor. The magnitude of this factor depends upon the magnification coefficient of the lenses placed between the aperture and the specimen.

On the basis of (9) and (11), we obtain an expression correlating the mutual intensity on the entrance surface of the specimen and that on plane  $B$  in the case of slight deviations from the normal incidence of the electron beam. The expression remains valid for any type of illumination and has the form

$$J_c(\mathbf{r}_{c1}, \mathbf{r}_{c2}) = J_0(\mathbf{r}_{c1}, \mathbf{r}_{c2}) \exp[2\pi i \mathbf{k}_0 \cdot (\mathbf{r}_{c1} - \mathbf{r}_{c2})], \quad (15)$$

where  $J_0(\mathbf{r}_{c1}, \mathbf{r}_{c2}) \simeq J_B(\boldsymbol{\mu}_{B1}, \boldsymbol{\mu}_{B2})$ ,  $\boldsymbol{\mu}_{Bi}$  is the projection of vector  $\mathbf{r}_{ci}$  on plane  $B$ , and  $\mathbf{k}_0$  is the vector parallel to the optical axis of the microscope whose modulus is  $k_0 = 1/\lambda_0$ .

### 3. Mutual intensity at exit from crystal

#### 3.1. General case

To describe the propagation of mutual intensity through the crystal, first we find the relationship between the wavefunctions of a separate electron on its entrance and exit surfaces. For simplicity, we assume the zero Laue zone for an incident beam of electrons to be parallel to the entrance surface of the crystal and coincident with plane  $k_x 0 k_y$ . Since the Bloch-wave method will be used for the description of electron scattering in a crystal, it is reasonable to present  $\Psi_V(\mathbf{r}, t, i)$  in a vacuum near the crystal as a superposition of de Broglie waves:

$$\Psi_V(\mathbf{r}, t, i) = \iint \tilde{A}(\mathbf{k}, E, i) \exp[2\pi i(\mathbf{k} \cdot \mathbf{r} - Et/h)] d\mathbf{k} dE, \quad (16)$$

where  $\tilde{A}(\mathbf{k}, E, i)$  is the wave amplitude and the modulus of wave vector  $\mathbf{k}$  is  $k(E) = 1/\lambda(E)$ .

For each value of energy  $E$ , the longitudinal  $k_z$  component of the wave vector can be expressed in terms of its transverse components. Thus, we have

$$\tilde{A}(\mathbf{k}, E, i) = \tilde{A}(\mathbf{p}, E, i) \delta[k_z - k_z(\mathbf{p}, E)], \quad (17)$$

where  $k_z(\mathbf{p}, E) = [k^2(E) - p^2]^{1/2}$ , and  $\mathbf{p}$  is the projection of vector  $\mathbf{k}$  onto plane  $k_x 0 k_y$ .

We write the electron wavefunction in the crystal as

$$\Psi(\mathbf{r}, t, i) = \int \Psi_S(\mathbf{r}, E, i) \exp(-2\pi i Et/h) dE. \quad (18)$$

Functions  $\Psi_S(\mathbf{r}, E, i)$  describing the stationary states with energy  $E$  can be found from the Schrödinger equation where relativistic corrections have been introduced. For the incident electron wave (16),  $\Psi_S(\mathbf{r}, E, i)$  can be presented as a superposition of the Bloch-wave packages (Borgardt, 1993b)

$$\Psi_S(\mathbf{r}, E, i) = \sum_j \int \Psi^{(j)}(\mathbf{p}, E, i) b^{(j)}(\mathbf{p}, \mathbf{r}, E) d\mathbf{p}, \quad (19)$$

where

$$b^{(j)}(\mathbf{p}, \mathbf{r}, E) \equiv b^{(j)}(\mathbf{k}_0^{(j)}, \mathbf{r}, E) \\ = \exp(2\pi i \mathbf{k}_0^{(j)} \cdot \mathbf{r}) \sum_g C_g^{(j)}(\mathbf{p}, E) \exp(2\pi i \mathbf{g} \cdot \mathbf{r}),$$

$b^{(j)}(\mathbf{p}, \mathbf{r}, E)$  is the  $j$ th Bloch wave excited in a crystal by a plane incident wave with energy  $E$  and a transverse component of wave vector  $\mathbf{p}$ .  $\Psi^{(j)}(\mathbf{p}, E, i)$  is the excitation amplitude of this wave,  $\mathbf{k}_0^{(j)}$  is the vector with components  $[p_x, p_y, k_{0z}^{(j)}(\mathbf{p}, E)]$  and  $\mathbf{g}$  is a reciprocal-lattice vector.

Periodicity of the Bloch-wave functions on reciprocal space makes it possible to select transverse components of all physically distinguished Bloch waves within the region  $\Omega_0$ , which is the cross section of the Wigner-Seitz cell of the reciprocal lattice on the plane  $k_x 0 k_y$ . This region is a two-dimensional Brillouin zone whose center it is expedient to bring into coincidence with point  $(p_{0x} = k_{0x}, p_{0y} = k_{0y})$ . Variations of the wavefunction produced by inelastic scattering can be taken into account by adding small imaginary parts to the  $k_z$  components of wave vectors  $\mathbf{k}_0^{(j)}$  (Hirsch, Howie, Nicholson, Pashley & Whelan, 1965).

For fast electrons incident on the crystal in the directions close to the normal to the surface, the boundary conditions are reduced to the equality of wavefunctions on plane  $z = z_c = 0$ . Using (16) and (17), we present  $\Psi_V(\mathbf{r}_c, t, i)$  in the form

$$\Psi_V(\mathbf{r}_c, t, i) = \sum_g \iint_{\Omega_0} \tilde{A}(\mathbf{p}' + \mathbf{g}_p, E, i) \\ \times \exp\{2\pi i[(\mathbf{p}' + \mathbf{g}_p) \cdot \boldsymbol{\rho}_c - Et/h]\} d\mathbf{p}' dE,$$

where  $\mathbf{g}_p$  is the projection of vector  $\mathbf{g}$  on the plane  $k_x 0 k_y$  and  $\boldsymbol{\rho}_c$  is a vector in the plane  $x 0 y$  with components  $\rho_{cx} = x_c, \rho_{cy} = y_c$ .

From the usual calculations (see *e.g.* Jones, Rackham & Steeds, 1977) for amplitudes  $\Psi^{(j)}$ , we obtain

$$\Psi^{(j)}(\mathbf{p}', E, i) = \sum_g \tilde{A}(\mathbf{p}' + \mathbf{g}_p, E, i) C_g^{(j)*}(\mathbf{p}', E) (1 + g_z/K), \quad (20)$$

where  $\mathbf{p}' \in \Omega_0$ ,  $K(E) = [k^2(E) + U_0]^{1/2}$  and  $U_0$  is the normalized mean crystal potential.

Since the magnitude of  $\delta E$  is small, in the calculation of  $\Psi(\mathbf{r}, t, i)$  we can assume that

$$C_g^{(j)}(\mathbf{p}, E) \simeq C_g^{(j)}(\mathbf{p}, E_i), \quad (21)$$

$$k_{0z}^{(j)}(\mathbf{p}, E) \simeq k_{0z}^{(j)}(\mathbf{p}, E_i) + (E - E_i)/[h v_z^{(j)}(\mathbf{p}, E_i)], \quad (22)$$

where  $v_z^{(j)} = (1/h) \partial E / \partial \text{Re}(k_{0z}^{(j)})$  is the  $z$  component of the electron velocity for the  $j$ th branch while variations of the imaginary part  $k_{0z}^{(j)}$  are considered negligible.

Then, substituting (19) and (20) into (18) and taking into account (21) and (22), for the electron wavefunction we obtain

$$\begin{aligned} \Psi(\mathbf{r}, t, i) = & \sum_j \sum_g \int \int_{\Omega_0} \Psi[\mathbf{r}_c, t - z/v_z^{(j)}(\mathbf{p}, E_i), i] \\ & \times C_g^{(j)*}(\mathbf{p}, E_i) [1 + g_z/K(E_i)] b^{(j)}(\mathbf{p}, \mathbf{r}, E_i) \\ & \times \exp\{-2\pi i[E_i t/hv_z^{(j)}(\mathbf{p}, E_i)]\} \\ & \times \exp[-2\pi i(\mathbf{p} + \mathbf{g}_p) \cdot \boldsymbol{\rho}_c] d\boldsymbol{\rho}_c d\mathbf{p}. \end{aligned} \quad (23)$$

Using (23), we find mutual intensity at points  $\mathbf{r}_{e1}$  and  $\mathbf{r}_{e2}$  on the entrance surface of the crystal. While doing this, we shall assume that (21) is valid at  $E = E_0$  for all electrons of the beam and take into account that in the cases of interest the following relationship is satisfied:

$$\begin{aligned} & |[z_{e1}/v_z^{(j)}(\mathbf{p}_1, E_i)] - [z_{e2}/v_z^{(j)}(\mathbf{p}_2, E_i)]| \\ & \simeq |z_{e1} - z_{e2}|/[v_z(\mathbf{p}_0, E_0)] \ll \tau_c, \end{aligned}$$

where  $v_z(\mathbf{p}_0, E_0)$  is the  $z$  component of the electron velocity in a vacuum.

Substituting (23) into (1) and taking (2) into account, we obtain an expression correlating the mutual intensity on the entrance and exit surfaces of the crystal under partially coherent illumination

$$\begin{aligned} J_e(\mathbf{r}_{e1}, \mathbf{r}_{e2}) = & \sum_j \sum_l \sum_{g_1} \sum_{g_2} \iiint \int_{\Omega_0 \Omega_0} J_c(\mathbf{r}_{c1}, \mathbf{r}_{c2}) C_{g_1}^{(j)*}(\mathbf{p}_1) \\ & \times C_{g_2}^{(l)}(\mathbf{p}_2) (1 + g_{1z}/K) (1 + g_{2z}/K) \\ & \times b^{(j)}(\mathbf{p}_1, \mathbf{r}_{e1}) b^{(l)*}(\mathbf{p}_2, \mathbf{r}_{e2}) \\ & \times \exp[-2\pi i(\mathbf{p}_1 + \mathbf{g}_{1p}) \cdot \boldsymbol{\rho}_{c1}] \\ & \times \exp[2\pi i(\mathbf{p}_2 + \mathbf{g}_{2p}) \cdot \boldsymbol{\rho}_{c2}] d\boldsymbol{\rho}_{c1} d\boldsymbol{\rho}_{c2} d\mathbf{p}_1 d\mathbf{p}_2, \end{aligned} \quad (24)$$

where functions depending on energy are calculated at  $E = E_0$ .

Expressions (23) and (24) determine the electron wave functions and mutual intensity for incident beams of an arbitrary divergence. Its constituent Bloch functions can be determined analytically in a two-beam approximation and for certain symmetrical orientations (Hirsch *et al.*, 1965). In the general case, they are calculated with the help of numerical methods. One of the programs for such calculations has been suggested by Zuo, Gjonnes & Spence (1989). In the following sections, for simplification of formulae we restrict ourselves to considering the scattering of electron waves with a divergency at which there is no overlapping between the intensity discs in a diffraction pattern. In this case, in expressions (23) and (24) the components with  $\mathbf{g}_1 = \mathbf{g}_2 = 0$  are non-zero and denoting the integration region  $\Omega_0$  with respect to  $\mathbf{p}_1$  and  $\mathbf{p}_2$  can be omitted since the expressions under the integral sign outside this region are equal to zero.

### 3.2. Scattering of beams with a small divergency

The influence of the illumination coherence upon the intensity distribution on the exit surface is easily understood if we analyze the scattering of beams with a small divergency in a crystal. In this case, wave vectors of de Broglie waves make a small angle with the optic axis of the microscope. Hence, on the branches of dispersion surfaces, points in the vicinity of  $\mathbf{p}_0$  are excited. Therefore, in the calculation of (24) we can assume that

$$C_g^{(j)}(\mathbf{p}) \simeq C_g^{(j)}(\mathbf{p}_0). \quad (25)$$

If the crystal is not excessively thick, then in the expansion  $k_z$  of the component of the wave vectors into the Taylor series in the vicinity of  $\mathbf{p}_0$  we can retain the terms up to the linear one with respect to  $(\mathbf{p} - \mathbf{p}_0)$ , *i.e.*

$$k_{0z}^{(j)}(\mathbf{p}) \simeq k_{0z}^{(j)}(\mathbf{p}_0) + \boldsymbol{\alpha}^{(j)} \cdot (\mathbf{p} - \mathbf{p}_0), \quad (26)$$

where  $\boldsymbol{\alpha}^{(j)} = \partial \text{Re } k_{0z}^{(j)} / \partial \mathbf{p}$ , and variations of imaginary parts  $k_{0z}^{(j)}$  are not taken into account.

Using (3), (15) and (24) and taking into account (25) and (26), for the intensity on the crystal exit surface we have

$$\begin{aligned} I(\mathbf{r}_e) = & \sum_j \sum_l \sum_{g_1} \sum_{g_2} J_0[(\boldsymbol{\rho}_e + \Delta\boldsymbol{\rho}_e^{(j)}, z_c), (\boldsymbol{\rho}_e + \Delta\boldsymbol{\rho}_e^{(l)}, z_c)] \\ & \times C_0^{(j)*} C_0^{(l)} C_{g_1}^{(j)} C_{g_2}^{(l)*} \\ & \times \exp[2\pi i(\mathbf{k}_0^{(j)} + \mathbf{g}_1 - \mathbf{k}_0^{(l)*} - \mathbf{g}_2) \cdot \mathbf{r}_e], \end{aligned} \quad (27)$$

where  $\Delta\boldsymbol{\rho}_e^{(j)} = \boldsymbol{\alpha}^{(j)} z_e$ ,  $\boldsymbol{\rho}_e$  is the projection of vector  $\mathbf{r}_e$  on plane  $xOy$ , while values  $C_g^{(j)}$  and  $\mathbf{k}_0^{(j)}$  correspond to  $\mathbf{p} = \mathbf{p}_0$ .

Unlike the expression for intensity obtained in the incident-plane-wave approximation, (27) includes function  $J_0$ , which has its maximum magnitudes when its arguments are equal. If the electron waves illuminating the crystal excite sections of the dispersion surface that are not parallel to one another, the value  $s_e^{(j)} = |\Delta\boldsymbol{\rho}_e^{(j)} - \Delta\boldsymbol{\rho}_e^{(l)}|$  is increased at  $j \neq l$  with the crystal thickness growing. This implies a relative decrease of the contribution of the corresponding term in (27). In cases when  $s_e^{(j)}$  begins to exceed the coherence length  $l_s$  of the incident electron beam, its contribution becomes small, and hence the Bloch-wave packages of the  $j$ th and  $l$ th branches lose their ability for constructive interference. The manifestation of this effect for a crystal with a definite orientation depends upon its thickness and the coherence length  $l_s$ . To explain this, it is necessary to take into account that the disturbances are transferred by the Bloch-wave packages in directions perpendicular to the excited sections of the dispersion surfaces (Borgardt, 1993b). One can become certain of the validity of this regularity if in calculation of (23) one uses relationships (25) and (26). Hence, the constructive interference of Bloch waves of the  $j$ th and  $l$ th branches at point  $\mathbf{r}_e$  depends

upon correlation of the incident electron waves at points  $\mathbf{r}_{c1}$  and  $\mathbf{r}_{c2}$  spaced at  $s_e^{(j)}$ .

If the divergence is not small, approximations (25) and (26) become insufficient. In these cases, the intensity on the exit surface will not only depend on the tilt of the excited sections of the dispersion surface but on their curvature and also on variation of coefficients  $C_g^{(j)}$  in the vicinity of point  $(p_{0x}, p_{0y})$ .

### 3.3. Incoherent illumination

According to (15) and (24), to determine mutual intensity on the exit surface of the crystal it is necessary to calculate the magnitude of integrals

$$\mathcal{I} = \iint J_B(\boldsymbol{\mu}_{B1}, \boldsymbol{\mu}_{B2}) \exp[-2\pi i(\mathbf{p}_1 - \mathbf{p}_0) \cdot \boldsymbol{\rho}_{c1}] \times \exp[2\pi i(\mathbf{p}_2 - \mathbf{p}_0) \cdot \boldsymbol{\rho}_{c2}] d\boldsymbol{\rho}_{c1} d\boldsymbol{\rho}_{c2}. \quad (28)$$

We introduce a new variable  $\boldsymbol{\rho}'_c = \boldsymbol{\rho}_{c1} - \boldsymbol{\rho}_{c2}$ . Then, after substituting (12) and (13) into (28) and taking into consideration that the angle between the entrance surface of the crystal and plane  $B$  is small, we use the relationships

$$\boldsymbol{\mu}_{B1} - \boldsymbol{\mu}_{B2} \simeq \boldsymbol{\rho}'_c, \quad \boldsymbol{\mu}_{B1}^2 - \boldsymbol{\mu}_{B2}^2 \simeq 2\boldsymbol{\rho}'_c \cdot \boldsymbol{\rho}_{c2} + (\boldsymbol{\rho}'_c)^2, \\ \mathbf{p}_1 \cdot \boldsymbol{\rho}_{c1} - \mathbf{p}_2 \cdot \boldsymbol{\rho}_{c2} = \mathbf{p}_1 \cdot \boldsymbol{\rho}'_c + (\mathbf{p}_1 - \mathbf{p}_2) \cdot \boldsymbol{\rho}_{c2}.$$

Since under incoherent illumination the coherence length  $l_s$  is much smaller than the size of the illuminated region, we can also assume

$$s_B(\boldsymbol{\mu}_{B1}) \simeq s_B(|\boldsymbol{\rho}'_c + \boldsymbol{\rho}_{c2}|) \simeq s_B(\boldsymbol{\rho}_{c2}), \\ \exp[\pi i(\boldsymbol{\rho}'_c)^2 / \lambda_0 z_a] = \exp[i(\boldsymbol{\rho}'_c)^2 / 2l_s d_a] \simeq 1.$$

Taking into account the above remarks, we have

$$\mathcal{I} = (I_B/\pi)(\lambda_0 z_a/d_a)^2 \int s_a(|\boldsymbol{\mu} - (\mathbf{p}_1 - \mathbf{p}_0)\lambda_0 z_a|) s_B(\boldsymbol{\mu}) \times \exp[-2\pi i(\mathbf{p}_1 - \mathbf{p}_2) \cdot \boldsymbol{\mu}] d\boldsymbol{\mu}. \quad (29)$$

The expression obtained is non-zero if the circles with centers at the origin of coordinates and at the point determined by vector  $(\mathbf{p}_1 - \mathbf{p}_0)\lambda_0 z_a$  have a common region. This is true for vectors  $\mathbf{p}_1$  satisfying the condition

$$|\mathbf{p}_1 - \mathbf{p}_0| \leq d_a/\lambda_0 z_a + d_B/\lambda_0 z_a \simeq k_0 \theta_a, \quad (30)$$

where it is taken into account that the radius of the source image is many times smaller than that of the aperture.

Since for almost all values of vector  $\mathbf{p}_1$  the range of integration in (29) is determined by function  $s_B(\boldsymbol{\mu})$ , we obtain for  $\mathcal{I}$

$$\mathcal{I} \simeq I_B(\lambda_0 z_a d_B/d_a)^2 [2J_1(2\pi d_B |\mathbf{p}_1 - \mathbf{p}_2|) / 2\pi d_B |\mathbf{p}_1 - \mathbf{p}_2|] \times S_a(|\mathbf{p}_1 - \mathbf{p}_0|), \quad (31)$$

where  $S_a(p)$  is the form function in the reciprocal space, whose appearance is determined by (30). It is equal to unity at  $p \leq k_0 \theta_a$  and to zero at other values of  $p$ .

From (31) it follows that  $\mathcal{I}$  becomes small at  $|\mathbf{p}_1 - \mathbf{p}_2| \gtrsim 1/d_B$ . Under incoherent illumination, the radius of the spot is far in excess of the lattice parameter. Therefore, in calculation of the mutual intensity, wave vector  $\mathbf{k}_g^{(j)}$  and coefficients  $C_g^{(j)}$  at point  $\mathbf{p}_1$  can be approximately expressed in terms of their values at point  $\mathbf{p}_2$  using relationships similar to (25) and (26). Then, substituting (29) into (24) and taking into account (30), after transformation we find

$$J_e(\mathbf{r}_{e1}, \mathbf{r}_{e2}) = (I_B/\pi)(\lambda_0 z_a/d_a)^2 \sum_j \sum_l \int s_B(|\boldsymbol{\rho}_{e1} + \mathbf{a}^{(j)} z_{e1}|) \times S_a(|\mathbf{p} - \mathbf{p}_0|) C_0^{(j)*}(\mathbf{p}) C_0^{(l)}(\mathbf{p}) b^{(j)}(\mathbf{p}, \mathbf{r}_{e1}) \times b^{(l)*}(\mathbf{p}, \mathbf{r}_{e2}) d\mathbf{p}.$$

Hence, for intensity at points not lying in the vicinity of the image edge, we have

$$I_e(\mathbf{r}_e) = \int I_{ep}(\mathbf{r}_e, \mathbf{p}) S_a(|\mathbf{p} - \mathbf{p}_0|) d\mathbf{p}, \quad (32)$$

where  $I_{ep}(\mathbf{r}_e, \mathbf{p})$  is the intensity at point  $\mathbf{r}_e$  determined by the incident plane wave with the wave vector transverse component equal to  $\mathbf{p}$ .

Formula (32) is the basis of the frequently used approach that the passage of an electron beam through a perfect crystal can be described as scattering of independent plane waves falling onto it at different angles. This approach is valid when the illumination system is focused on plane  $B$ . If the electron source image is located higher or lower than the specimen entrance surface, then, according to Pozzi (1987), coherence length  $l_s$  increases and (12) and (13) cannot be used for calculations of mutual intensity.

## 4. Transmitted-electron-beam intensity for a wedge-shaped crystal

At the end of §3.2, we noted that under partially coherent illumination the constructive interference of Bloch waves of different branches of the dispersion surface can be suppressed. As an illustration of this effect, we shall consider a case of the intensity distribution in the images with a diffraction contrast of a wedge-shaped crystal. The intensity thickness oscillations in such images appear as a result of the constructive interference of Bloch waves of different branches. Therefore, variations in the oscillation amplitude give an insight into the effect of the illumination coherence on the interference of those waves.

For simplicity, we assume the edge of the wedge to be parallel to axis  $y$  and then obtain the expression for mutual intensity on plane  $D$  perpendicular to the microscope optical axis (Fig. 2a). In this section, we shall consider only diffraction from the zero Laue zone ( $\mathbf{g}_p = \mathbf{g}$ ) and assume that the shape of the crystal specimen has no effect on the lattice potential, and make use of expression (19) for wavefunctions. In the frame-

work of this approach, it is impossible to describe Fresnel contrast of the specimen edge; this is, however, not essential for the current analysis.

The wavefunction of each electron after emerging from the crystal is the sum of the transmitted and diffracted waves and can be written as

$$\Psi_T(\mathbf{r}, t, i) = \sum_j \sum_{\mathbf{g}'} \iint \tilde{B}_{\mathbf{g}'}^{(j)}(\mathbf{p}' + \mathbf{g}', E, i) \times \exp[2\pi i(\boldsymbol{\kappa}_{\mathbf{g}'} \cdot \mathbf{r} - Et/h)] d\mathbf{p}' dE, \quad (33)$$

where  $\boldsymbol{\kappa}_{\mathbf{g}'} = [\mathbf{p}' + \mathbf{g}', \kappa_z(\mathbf{p}' + \mathbf{g}', E)]$  is the wave vector of an electron wave in a vacuum in a stationary state with energy  $E$ .

If the reflection of waves when they leave the crystal is neglected, the boundary conditions reduce to the equality of the wavefunctions on its exit surface

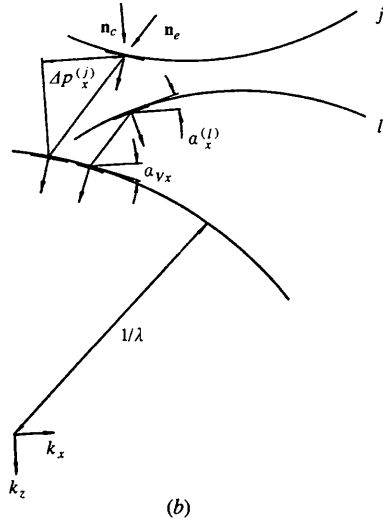
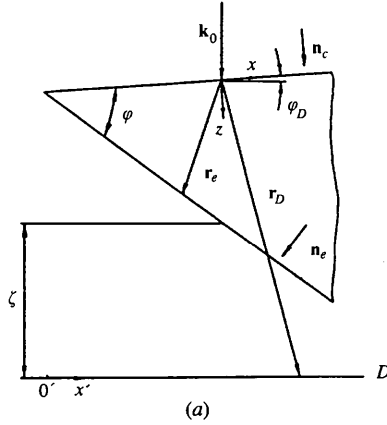


Fig. 2. Cross sections of a wedge-shaped crystal (a) and of the corresponding dispersion surface (b).  $\mathbf{n}_c$  and  $\mathbf{n}_e$  are normals to the entrance and exit surfaces of the crystal. The excited sections on the dispersion surface and on the sphere of equal energy in a vacuum can be seen in (b). Arrows in (b) show the directions in which electron waves transfer disturbances.

$$\Psi_T(\mathbf{r}_e, t, i) = \Psi(\mathbf{r}_e, t, i), \quad (34)$$

and the components of vector  $\mathbf{r}_e$  are correlated by the relationship

$$z_e = x_e \tan \varphi + z_0,$$

where  $x_e \geq -z_0 \cot \varphi$ ,  $\varphi$  is an angle of the wedge and  $z_0$  is the crystal thickness at point  $x = 0$ .

Having used (18), (19) and (33), we can see that (34) is true only for transverse components  $\mathbf{p}'$ ,  $\mathbf{g}'$  and  $\mathbf{p}$ ,  $\mathbf{g}$  of wave vectors in a vacuum, and in the crystal the following relationships are valid:

$$p'_y = p_y, \quad \mathbf{g}' = \mathbf{g},$$

$$p'_x + \kappa_z(\mathbf{p}' + \mathbf{g}', E) \tan \varphi = p_x + k_{0z}^{(j)}(\mathbf{p}, E) \tan \varphi.$$

These equations simply imply that the projections of wave vectors onto the crystal exit surface in transition of the plane electron wave from the crystal to vacuum are invariable (Fig. 2b). Since the differences between  $p'_x$  and  $p_x$  are small, the value of  $\kappa_z$  in the vicinity of point  $(\mathbf{p} + \mathbf{g})$  can be presented as the first two terms of the Taylor series. Then for  $\mathbf{p}'$  we obtain

$$\mathbf{p}' = \mathbf{p} + \Delta\mathbf{p}^{(j)}(\mathbf{p}, \mathbf{g}, E),$$

where

$$\Delta p_x^{(j)}(\mathbf{p}, \mathbf{g}, E) \simeq [k_{0z}^{(j)}(\mathbf{p}, E) - \kappa_z(\mathbf{p} + \mathbf{g}, E)][1 + \alpha_T \tan \varphi]^{-1} \times \tan \varphi,$$

$$\Delta p_y^{(j)}(\mathbf{p}, \mathbf{g}, E) = 0,$$

$$\alpha_T = -(p_x + g_x)/\kappa_z(\mathbf{p} + \mathbf{g}, E).$$

Taking into account the expressions obtained from (34), we can find amplitudes  $\tilde{B}_{\mathbf{g}}^{(j)}$ . Proceeding as shown in §3.1, it is possible to obtain an expression for the wave functions of electrons, and on this basis to calculate the mutual intensity of an electron beam after scattering in the crystal:

$$J_T(\mathbf{r}_1, \mathbf{r}_2) = \sum_j \sum_l \sum_{\mathbf{g}_1} \sum_{\mathbf{g}_2} \iiint J_c(\mathbf{r}_{c1}, \mathbf{r}_{c2}) C_0^{(j)*}(\mathbf{p}_1) \times C_{\mathbf{g}_1}^{(j)}(\mathbf{p}_1) C_0^{(l)}(\mathbf{p}_2) C_{\mathbf{g}_2}^{(l)*}(\mathbf{p}_2) \exp\{2\pi i[k_{0z}^{(j)}(\mathbf{p}_1) - k_{0z}^{(l)*}(\mathbf{p}_2)]z_0\} \exp\{2\pi i[\kappa_z(\mathbf{p}_1 + \mathbf{g}_1 + \Delta\mathbf{p}^{(j)}) \times (z_1 - z_0) - \kappa_z(\mathbf{p}_2 + \mathbf{g}_2 + \Delta\mathbf{p}^{(l)})(z_2 - z_0)]\} \times \exp\{2\pi i[(\mathbf{p}_1 + \mathbf{g}_1 + \Delta\mathbf{p}^{(j)}) \cdot \boldsymbol{\rho}_1 - (\mathbf{p}_2 + \mathbf{g}_2 + \Delta\mathbf{p}^{(l)}) \cdot \boldsymbol{\rho}_2]\} \times \exp[-2\pi i(\mathbf{p}_1 \cdot \boldsymbol{\rho}_{c1} - \mathbf{p}_2 \cdot \boldsymbol{\rho}_{c2})] \times d\boldsymbol{\rho}_{c1} d\boldsymbol{\rho}_{c2} d\mathbf{p}_1 d\mathbf{p}_2, \quad (35)$$

where all the values depending upon the energy are calculated at  $E = E_0$ .

The expression obtained determines the mutual intensity of the electron beam after scattering in a wedge-shaped crystal. Using the expression as the base,



according to Dinges, Berger & Rose (1995) we can calculate mutual intensity on the image plane taking into account the transfer function of the microscope. However, if we restrict ourselves to consideration of beams with a small divergency, calculations of the intensity of the transmitted or one of the diffracted beams are essentially simplified. In this case, the effect of spherical aberration and the finite size of the objective aperture can be neglected. As a result, the intensity distribution on plane  $D$  and that in the image differ only in the scale factor.

To determine the transmitted-beam intensity  $[I_0(\mathbf{r}_D)]$  on the plane of the objective-lens focus, it is sufficient to group terms with  $\mathbf{g}_1 = \mathbf{g}_2 = 0$  and assume  $\mathbf{r}_1 = \mathbf{r}_2 = \mathbf{r}_D$  in (35). We shall carry out calculations in a two-beam approximation for an Si crystal and electrons with 100 keV kinematic energy. We assume that  $p_{0y} = 0$  and vector  $\mathbf{g}$  corresponding to the reflection on plane (220) is directed along axis  $x$ . Values  $C_g^{(j)}$  and  $k_{0z}^{(j)}$  are determined according to formulae presented *e.g.* in Hirsch *et al.* (1965). Using the expression for  $k_{0z}^{(j)}$  as a base, value  $\alpha_x^{(j)}$  can be presented as

$$\alpha_x^{(j)} = -[(-1)^j w \tan \theta_B] / [(1 + w^2)^{1/2}],$$

where  $w = -(2p_{0x} + g)\xi_g \tan \theta_B$ ,  $\xi_g$  is the extinction length and  $\theta_B$  the Bragg angle equal to  $\theta_B \simeq g/2k_0$ .

According to Hirsch *et al.* (1965), the extinction length is  $\xi_g = 75.7$  nm, while the absorption lengths and the mean inner potential according to Radi (1970) are  $\xi'_0 = 0.6/\xi_g$ ,  $\xi'_g = 0.025/\xi_g$  and  $V_0 = 11.85$  eV, respectively.

Under incoherent illumination, mutual intensity on the crystal entrance surface is determined using (12), (14) and (15). In the calculations, distance  $z_a$  was taken to be equal to 251.4 nm, which conforms with microscope JEM-100C (Spence, 1988). It implies that with the aperture size  $d_a = 200$   $\mu\text{m}$ , angle  $\theta_a \simeq 4 \times 10^{-4}$  rad, while the coherence length  $l_s \simeq 1.5$  nm.

At a small divergency of the incident beam for  $k_{0z}^{(j)}$  and  $C_g^{(j)}$  in the vicinity of  $\mathbf{p}_0$ , we can use (25) and (26) and present value  $\Delta p_x^{(j)}$  as

$$\Delta p_x^{(j)}(\mathbf{p}) \simeq \Delta p_x^{(j)}(\mathbf{p}_0) + [\partial \Delta p_x^{(j)}(\mathbf{p}_0)] / \partial p_x(\mathbf{p} - \mathbf{p}_0)_x.$$

When calculating the differences between the  $k_z$  components of the wave vectors in a vacuum in (35), one should take into account (31) and the fact that for the incident beam  $p_{0y} = 0$ . Hence, in a wide range of defocusing we have

$$\begin{aligned} & \kappa_z[\mathbf{p}_1 + \Delta \mathbf{p}^{(j)}(\mathbf{p}_1)] - \kappa_z[\mathbf{p}_2 + \Delta \mathbf{p}^{(j)}(\mathbf{p}_2)] \\ & \simeq \kappa_z(\mathbf{p}_T^{(j)}) - \kappa_z(\mathbf{p}_T^{(l)}) + (\mathbf{p}_1 - \mathbf{p}_0)_x \alpha_{v_x}(\mathbf{p}_T^{(j)}) \eta^{(j)} \\ & \quad - (\mathbf{p}_2 - \mathbf{p}_0)_x \alpha_{v_x}(\mathbf{p}_T^{(l)}) \eta^{(l)}, \end{aligned}$$

where

$$\begin{aligned} \alpha_{v_x} &= \partial \kappa_z / \partial p_x, \quad \mathbf{p}_T^{(j)} = \mathbf{p}_0 + \Delta \mathbf{p}^{(j)}(\mathbf{p}_0), \\ \eta^{(j)} &= 1 + \partial \Delta p_x^{(j)}(\mathbf{p}_0) / \partial p_x. \end{aligned}$$

Taking into account the above approximations, we obtain for intensity

$$\begin{aligned} I_0(\mathbf{r}_D) &= \sum_j \sum_l J_0[(\rho_D + \Delta \rho_D^{(j)}, z_c), (\rho_D + \Delta \rho_D^{(l)}, z_c)] \\ & \times C_0^{(j)*} C_0^{(j)} C_0^{(l)*} C_0^{(l)} \exp[2\pi i(k_{0z}^{(j)} - k_{0z}^{(l)*})z_0] \\ & \times \exp\{2\pi i[\kappa_z(\mathbf{p}_T^{(j)}) - \kappa_z(\mathbf{p}_T^{(l)})](z_D - z_0)\} \\ & \times \exp[2\pi i(\Delta \mathbf{p}^{(j)} - \Delta \mathbf{p}^{(l)}) \cdot \rho_D], \end{aligned} \quad (36)$$

where

$$\begin{aligned} \Delta \rho_{Dx}^{(j)} &= \alpha_x^{(j)} z_0 + \alpha_{v_x}(\mathbf{p}_T^{(j)}) \eta^{(j)} (z_D - z_0) \\ & \quad + (\partial \Delta p_x^{(j)} / \partial p_x) \rho_{Dx}, \\ \Delta \rho_{Dy}^{(j)} &= 0 \end{aligned}$$

and  $\rho_D$  is the projection of vector  $\mathbf{r}_D$  on plane  $xOy$ .

In (36), all functions depending on  $\mathbf{p}$  except  $\kappa_z(\mathbf{p})$  and  $\alpha_{v_x}(\mathbf{p})$  are calculated at  $\mathbf{p} = \mathbf{p}_0$  while the components of vector  $\mathbf{r}_D$  are correlated by the relationship

$$z_D \simeq \rho_{Dx} \tan \varphi_D + z_0 + \zeta / \cos \varphi_D,$$

where  $\varphi_D$  is the angle between axis  $x$  and plane  $D$ , and  $\zeta$  is the defocusing (Fig. 2a).

Fig. 3 illustrates the intensity profiles for the transmitted beam on the focusing plane  $D$ , calculated by (36), and in the incident plane-wave approximation. In Figs. 3(a)–(d), plane  $D$  is directly under the crystal exit surface. In plotting the curves, axis  $O'x'$ , whose origin is coincident with the projection of the wedge edge on plane  $D$ , was used. The intensity of the incident beam on the crystal entrance surface was assumed to be equal to unity.

If the specimen is at the Bragg condition, the incident-beam divergency has no effect on the intensity distribution (Fig. 3a). This is because at  $w = 0$  the excited sections on the branches of the dispersion surface are parallel to each other [ $\alpha_x^{(j)} = \alpha_x^{(l)} = 0$ ].

If the Bragg conditions are not fulfilled, the tilts of the excited sections differ. Therefore, as the crystal thickness grows, the distance between the entrance surface points whose correlation determines the oscillation amplitude increases. Since the difference in the tilt angles increases with increasing  $|w|$ , the intensity oscillations shown in Fig. 3(c) become suppressed at smaller thicknesses than those shown in Fig. 3(b).

As the incident-beam divergence reduces, the coherence length increases. Since the constructive interference of the Bloch-wave packages depends upon the relationship of values  $l_s$  and  $s_D^{(j)} = |\Delta \rho_D^{(j)} - \Delta \rho_D^{(l)}|$ , the intensity oscillations shown in Fig. 3(d) become suppressed at greater thicknesses than those shown in Fig. 3(c).

Fig. 3(e) shows the intensity profiles for a defocused image. From comparison of Fig. 3(c) and Fig. 3(e), it follows that at defocusing the amplitude of the intensity oscillations reduces for small thicknesses and increases in the range of large thicknesses. This effect can be explained by the fact that, as defocusing grows, plane  $D$  conjugated with the microscope screen becomes distant from the crystal exit surface. In scattering by a wedge-shaped crystal, Bloch waves of different branches excite different sections on the constant energy sphere in a vacuum while electron waves transfer the disturbances perpendicular to those sections (Fig. 2*b*). Since their tilts are not the same, an additional term linearly dependent on  $\zeta$  appears in  $S_D^{(jl)}$ . The presence of this term is responsible for variations in the intensity distribution at defocusing.

The observed regularities of the effect of the illumination coherence on the intensity thickness oscillations in bright-field images remain valid also for

dark-field images. To carry out the necessary calculations, it is sufficient to select the incident-beam orientation so that the  $g$ th diffracted beam should propagate along the optical axis.

It is noteworthy that the contrast variations similar to those above can appear in the diffraction images of the stalking fault. In this case, Bloch-wave packages with various sets of transverse components of the wave vectors arise as a result of inter-branch scattering on the stalking fault. The contrast changes produced by variations of the incident divergency and defocusing were experimentally investigated by Borgardt, Eremeev & Maksimov (1988).

## 5. Conclusions

To describe scattering of electron quasi-monochromatic beams in a crystal under partially coherent illumination, the mutual coherency and mutual intensity functions

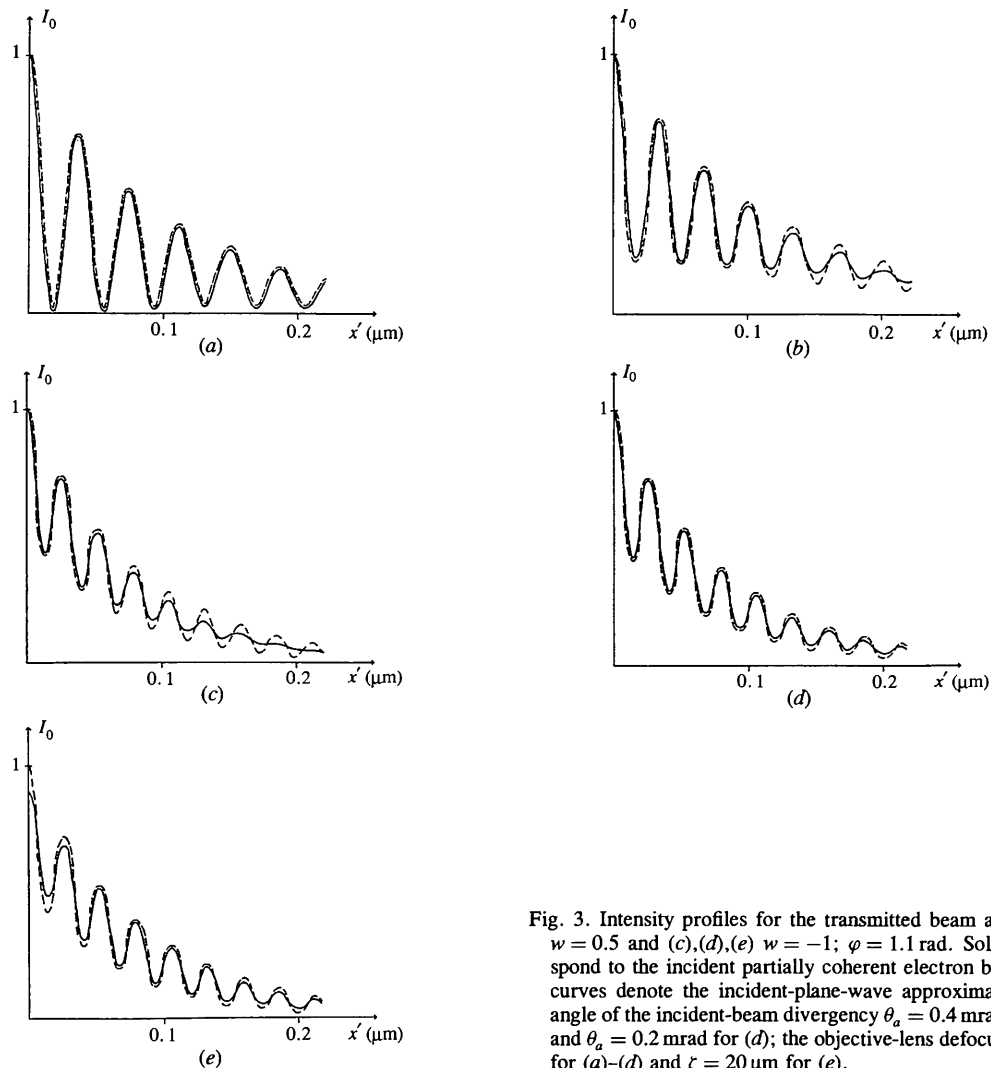


Fig. 3. Intensity profiles for the transmitted beam at (a)  $w = 0$ , (b)  $w = 0.5$  and (c), (d), (e)  $w = -1$ ;  $\varphi = 1.1$  rad. Solid curves correspond to the incident partially coherent electron beam, the dashed curves denote the incident-plane-wave approximation. The semi-angle of the incident-beam divergency  $\theta_a = 0.4$  mrad for (a)–(c), (e) and  $\theta_a = 0.2$  mrad for (d); the objective-lens defocusing  $\zeta = 0.3$   $\mu\text{m}$  for (a)–(d) and  $\zeta = 20$   $\mu\text{m}$  for (e).

were used. Although their definitions for electron waves differ from those accepted in optics, the functions allow a characterization of the electron beam as its optical analog.

To calculate the mutual intensity on the crystal exit surface, scattering of each electron by a specimen within the framework of the Bloch-wave formalism was described and then the coherent properties of an incident beam were taken into account. Such an approach made it possible to obtain an analytical expression correlating mutual intensities on the exit and entrance surfaces of a perfect crystal for a beam of arbitrary divergency.

On the basis of the formulae obtained, it is shown that the approach of plane waves filling the illumination cone can be used for calculating the electron intensity under incoherent illumination.

For finding the effect of the illumination coherence on the electron diffraction, the case of a small divergent incident beam has been considered. It has been found that the constructive interference of Bloch waves of different branches depends upon the correlations of the incident beam at different points on the crystal entrance surface. The distance between these points is proportional to the angle between the excited sections of the dispersion surface and the thickness of the crystal. If it exceeds the coherence length of the incident beam, the constructive interference of Bloch waves is suppressed.

To illustrate this effect, the intensity distributions of a transmitted beam for a wedge-shaped crystal have been calculated. If the incident electrons excite non-parallel sections on the dispersion surface, and the focusing plane of the objective lens is in the vicinity of the crystal exit surface, the intensity oscillation amplitude is reduced with the growing thickness. At defocusing, the contrast of the extinction fringes changes since for a wedge-shaped crystal Bloch waves of different branches excite different sections on the constant-energy sphere in a vacuum.

#### References

- Bithell, E. G., Donovan, P. E. & Stobbs, W. M. (1989). *Philos. Mag.* **A59**, 63–85.
- Blum, K. (1981). *Density Matrix Theory and Applications*. New York: Plenum.
- Boersch, H. (1954). *Z. Phys.* **139**, 115–146.
- Borgardt, N. I. (1993a). *Kristallografiya*, **38**, 25–33. (In Russian.)
- Borgardt, N. I. (1993b). *Philos. Mag.* **A68**, 453–470.
- Borgardt, N. I., Ereemeev, P. M. & Maksimov, S. K. (1988). *Izv. Akad. Nauk SSSR Ser. Fiz.* **52**, 1300–1305. (In Russian.)
- Born, M. & Wolf, E. (1968). *Principles of Optics*. Oxford: Pergamon Press.
- Chou, C. T., Preston, A. R. & Steeds, J. W. (1992). *Philos. Mag.* **A65**, 863–888.
- Coene, W., Van Dyck, D. & Van Landaut, J. (1986). *Optik (Stuttgart)*, **73**, 13–18.
- Cowley, J. M. (1975). *Diffraction Physics*. Amsterdam: North-Holland.
- Dinges, C., Berger, A. & Rose, H. (1995). *Ultramicroscopy*, **60**, 49–70.
- Dudarev, S. L., Peng, L.-M. & Whelan, M. J. (1993). *Phys. Rev. B*, **48**, 13408–13429.
- Dudarev, S. L. & Ryazanov, M. I. (1988). *Acta Cryst.* **A44**, 51–61.
- Fejes, P. L. (1977). *Acta Cryst.* **A33**, 109–113.
- Frank, J. (1973). *Optik (Stuttgart)*, **38**, 519–536.
- Goodman, J. W. (1985). *Statistical Optics*. New York: John Wiley.
- Hawkes, P. W. (1978). *Adv. Opt. Electron Microsc.* **7**, 101–184.
- Hirsch, P. B., Howie, A., Nicholson, R. B., Pashley, D. W. & Whelan, M. J. (1965). *Electron Microscopy of Thin Crystals*. London: Butterworth.
- Humphreys, C. J. & Spence, J. C. H. (1981). *Optik (Stuttgart)*, **58**, 125–144.
- Ishizuka, K. (1980). *Ultramicroscopy*, **5**, 55–65.
- Jones, P. M., Rackham, G. M. & Steeds, J. W. (1977). *Proc. R. Soc. London. Ser. A*, **354**, 197–222.
- Kagan, Yu. & Kononets, Yu. V. (1970). *Sov. Phys. JETP*, **31**, 124–141.
- Kagan, Yu. & Kononets, Yu. V. (1973). *Sov. Phys. JETP*, **37**, 530–538.
- Katerbau, K.-H. (1981). *Philos. Mag.* **A43**, 409–426.
- Landau, L. D. & Lifshitz, E. M. (1977). *Quantum Mechanics, Non-Relativistic Theory*. Oxford: Pergamon Press.
- Pozzi, G. (1987). *Optik (Stuttgart)*, **77**, 69–73.
- Radi, G. (1970). *Acta Cryst.* **A26**, 41–56.
- Rez, P. (1978). *Electron Diffraction 1927–1977*, edited by P. J. Dobson, J. B. Pendry & C. J. Humphreys. *Inst. Phys. Conf. Ser.* No. 41, 61–67.
- Rose, H. (1984). *Ultramicroscopy*, **15**, 173–192.
- Spence, J. C. H. (1988). *Experimental High-Resolution Electron Microscopy*. Oxford University Press.
- Spence, J. C. H. & Zuo, J. M. (1992). *Electron Microdiffraction*. New York: Plenum.
- Wade, R. H. & Frank, J. (1977). *Optik (Stuttgart)*, **49**, 81–92.
- Wright, A. G. & Bird, D. M. (1992). *Acta Cryst.* **A48**, 215–221.
- Zuo, J. M., Gjonnes, K. & Spence, J. C. H. (1989). *J. Electron Microsc. Tech.* **12**, 29–55.